Journal of Leather Science and Engineering

RESEARCH Open Access

Polycaprolactone strengthening keratin/bioactive glass composite scaffolds with double cross-linking networks for potential application in bone repair

Liying Sun[1,2], Shan Li[1,2], Kaifeng Yang[1,2], Junchao Wang[1,2], Zhengjun Li[1,2*] and Nianhua Dan[1,2]

Abstract

In this study, we aimed at constructing polycaprolactone (PCL) reinforced keratin/bioactive glass composite scaffolds with a double cross-linking network structure for potential bone repair application. Thus, the PCL-keratin-BG composite scaffold was prepared by using keratin extracted from wool as main organic component and bioactive glass (BG) as main inorganic component, through both cross-linking systems, such as the thiol-ene click reaction between abundant sulfhydryl groups of keratin and the unsaturated double bond of 3-methacryloxy propyltrimethoxy silane (MPTS), and the amino-epoxy reaction between amino groups of keratin and the epoxy group in (3-glycidoxymethyl) methyldiethoxysilane (GPTMS) molecule, along with introduction of PCL as a reinforcing agent. The success of the thiol-ene reaction was verified by the FTIR and ^{1}H-NMR analyses. And the structure of keratin-BG and PCL-keratin-BG composite scaffolds were studied and compared by the FTIR and XRD characterization, which indicated the successful preparation of the PCL-keratin-BG composite scaffold. In addition, the SEM observation, and contact angle and water absorption rate measurements demonstrated that the PCL-keratin-BG composite scaffold has interconnected porous structure, appropriate pore size and good hydrophilicity, which is helpful to cell adhesion, differentiation and proliferation. Importantly, compression experiments showed that, when compared with the keratin-BG composite scaffold, the PCL-keratin-BG composite scaffold increased greatly from 0.91 ± 0.06 MPa and 7.25 ± 1.7 MPa to 1.58 ± 0.21 MPa and 14.14 ± 1.95 MPa, respectively, which suggesting the strong reinforcement of polycaprolactone. In addition, the biomineralization experiment and MTT assay indicated that the PCL-keratin-BG scaffold has good mineralization ability and no-cytotoxicity, which can promote cell adhesion, proliferation and growth. Therefore, the results suggested that the PCL-keratin-BG composite scaffold has the potential as a candidate for application in bone regeneration field.

Keywords: Keratin, Bioactive glass, Polycaprolactone, Double cross-linking networks, Bone regeneration

*Correspondence: lizhengjun@scu.edu.cn
[1] National Engineering Research Center of Clean Technology in Leather Industry, Sichuan University, Chengdu, China
Full list of author information is available at the end of the article

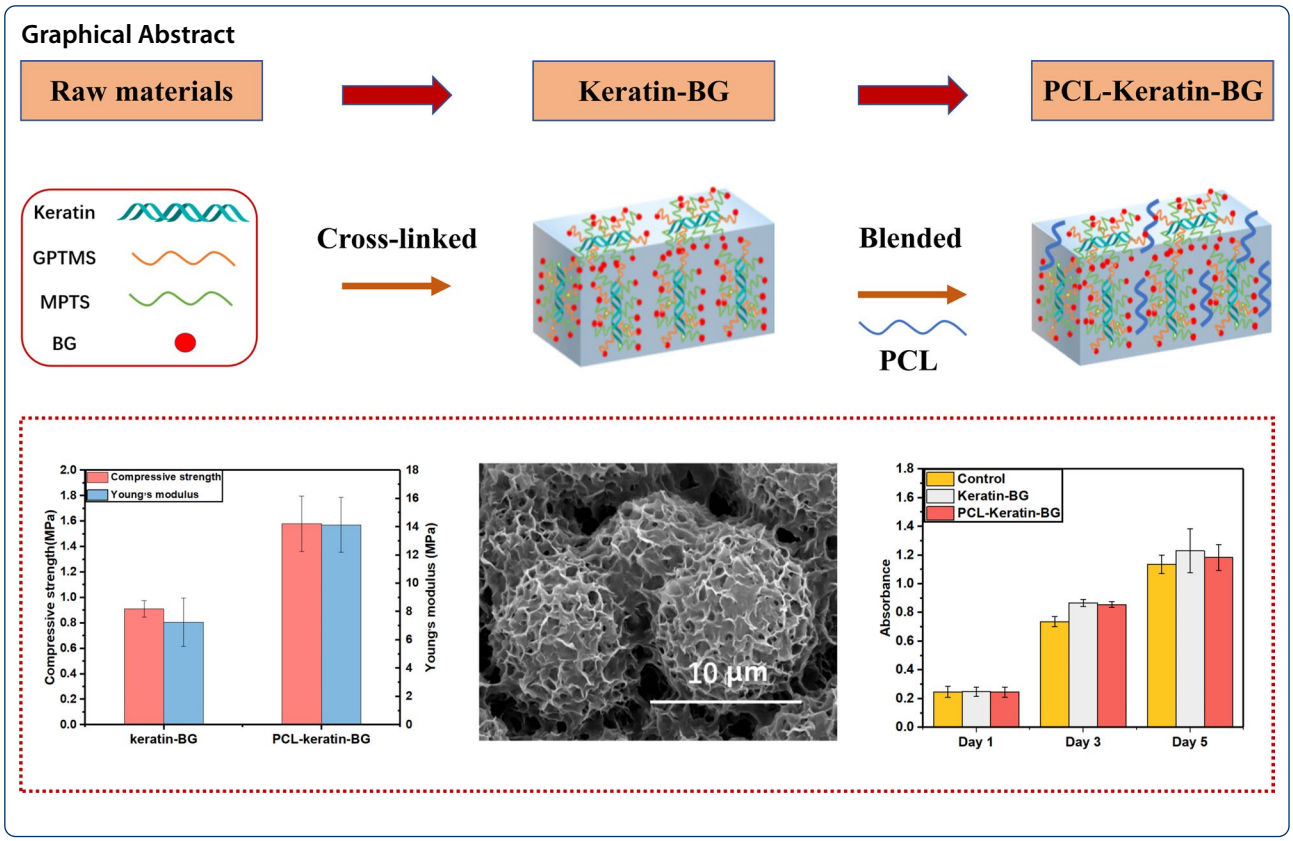

1 Introduction

In recent years, people pay more and more attention to bone defects due to traffic accidents, sports injuries and diseases [1–3]. Bone tissue engineering is promising and rapidly developing for application in bone repair, in which scaffold plays a crucial role by acting as a template for promoting the cell differentiation and growth within bone defects. In order to obtain scaffold materials with good biological properties to meet the requirements of bone regeneration, biomimetic bone composites containing inorganic and organic components are usually prepared by mimicking the chemical components in natural bones. Organic components used in general include natural polymers such as gelatin[4], collagen[5], sodium alginate [6] and chitosan [7–9], and synthetic polymers like polylactic acid [10], polyethylene glycol [11], poly(lactic-co-glycolic) acid [12] and polycaprolactone [13]. Among them, the preparation of composite bone scaffold materials based on collagen and its derivative gelatin is the most extensive and in-depth research [4, 14–16], because collagen is the main organic component of natural bone. Nevertheless, the high cost, poor mechanical strength, rapid degradation of collagen limit its practical applications. Therefore, it has become one of the important research directions to explore new alternative materials. In addition, polycaprolactone (PCL), as a synthetic polymer, is widely used to prepare composite scaffolds for bone repair [17, 18] because of its low cost, good mechanical properties and no toxicity. However, hydrophobicity and lack of functional groups that for cells growth and proliferation limit its interactions between cells. Fortunately, these problems could be solved by modifying PCL with hydrophilic materials to enhance its cell compatibility and bone regeneration ability [19]. Furthermore, as it is well known, the mechanical strength of scaffolds for bone repair is very important, but its great improvement is still a challenge. Therefore, it is worth noting that it is a good and promising strategy to combine the excellent cytocompatibility of hydrophilic natural polymer with the excellent mechanical properties of synthetic polymer.

Keratin, as the main component of wool, hair, nails hooves, feathers and horns, is one of the most abundant protein sources, and has found diverse applications [20]. It has biological activity and biodegradability and is a promising substitute for collagen which is usually used as an organic component for preparing bone repair scaffold materials. This is because that keratin has unique signal motifs, such as leucine-aspartic acid-valine (LDV) and glutamate-aspartic acid-serine (EDS) peptide domains,

which make cells adhere well [21], and keratin contains a large number of functional groups, such as amino group and carboxyl group, especially abundant intramolecular and intermolecular disulfide bonds, which provide active reaction sites for modification according to needs [22]. In recent years, Some researches on keratin-based scaffolds for bone tissue regeneration have been reported. For example, keratin/jellyfish collagen/hyaluronic acid scaffold prepared by freeze-drying method enabled better cell adhesive, improved the multilineage differentiation ability and cell proliferation, and had better osteointegration potential [22]. With poly(3-hydroxybutyrate) (PHB) and keratin as raw materials, the biomimetic scaffold with high porosity and hydrophilicity prepared by electrospinning exhibited improved hydrophilicity, in vitro degradability and significantly increased cell viability, which is due to the addition of keratin [23]. In addition, compared with the pure polylactic acid (PLA) membrane, the electrospun membrane using both keratin and PLA also showed improved cellular attraction owing to the addition of keratin [24]. Obviously, these reports prove that keratin is beneficial to improve the cell adhesion and hydrophilicity of composite scaffolds for bone repair. Interestingly, the existence of plenty of disulfide bonds and sulfhydryl groups offer more opportunities for keratin to be modified and functionalized by thiol-ene reaction [25]. The thiol-ene reaction can performed under mild reaction condition, is high efficiency and insensitivity to oxygen, and has high yield and no potential harmful by-products, therefore it is usually used in the field of biomedical materials [26–28]. For example, the surface of poly(globalide-*co*-ε-caprolactone) (PGlCL) nanoparticles containing double bonds can be functionalized with bovine serum albumin (BSA) by thiol-ene click chemistry, producing conjugates by covalently binding BSA to PGlCL [27]. In particular, Li [28] synthesized keratin-g-PEG copolymers through thiol-ene click chemistry using keratin extracted from wool and poly(ethylene glycol) methyl ether methacrylate (MPEGMA) catalyzed by potassium persulfate. Considering that 3-methacryloxypropyltrimethoxysilane (MPTS) has an alkenyl structure similar to MPEGMA, it is an electron-rich olefin, and for the thiol-ene click reaction, the reaction speed of electron-rich olefin is faster than that of electron-deficient olefin. Therefore, although few report on the thiol-ene click reaction of MPTS and keratin under the thermal initiator, it can be conceived that MPTS can undergo thiol-ene reaction with keratin, which will be performed in this study.

As for the inorganic component, hydroxyapatite is often used for preparing composite scaffolds for bone regeneration, because it is the main inorganic component of natural bone. However, bioactive glass (BG) has been proved to be an ideal inorganic component for preparing bone repair scaffolds [29], which has attracted great attention recently because of its excellent bioactivity, biocompatibility, biodegradability, bone bonding ability [30], and enhanced biomineralization ability to promote osseointegration and low biotoxicity [31]. Considering that the mechanical properties of bone repair scaffolds are one of the vital factors for new bone formation and reconstruction, and the improvement of interfacial compatibility between components in composites is helpful to enhance mechanical properties, therefore coupling agents with multi-functional groups are often used to solve the problems. For example, the porous composite scaffold (BG-Gel-CNC) constructed by freeze-drying technology exhibited improved mechanical properties, which is due to the use of γ-glycidoxypropyltrimethoxy silane (GPTMS), a silane couple agent, to enhance the compatibility among components including gelatin (Gel), cellulose nanocrystals (CNC) and bioactive glass (BG). The principle is that the epoxy groups in GPTMS molecule reacts with the amino groups in gelatin, and simultaneously the Si–OH groups produced by hydrolysis of Si-OR groups in GPTMS reacts with the Si–OH groups in BG [16]. Ziba Orshesh [32] also prepared gelatin/sodium alginate/45S5 BG scaffold using GPTMS as a cross-linking agent, and the similar results were obtained. Keratin contains lots of amino groups similar to collagen and its derivative gelatin. This strategy of using cross-linking agents such as GPTMS to enhance the interface interaction between inorganic and organic components and further improve mechanical properties could also be carried out when preparing composite scaffolds for bone repair.

On the other hand, PCL is widely used in bone tissue engineering to enhance the mechanical strength of scaffolds due to its good mechanical properties and biodegradability [33, 34], despite its limited cell affinity due to its hydrophobicity and lack of surface cell recognition sites. However, PCL-protein composite materials, when appropriately constructed, could integrate the favorable biological properties of protein and favorable mechanical properties of PCL [35–38]. Keratin-PCL composite nanofibers [37] fabricated by an electrospinning technique showed great increase in mechanical properties due to the introduction of PCL, and the larger the PCL content is, the stronger the mechanical strength. In other words, the Young's modulus and tensile strength breaking strength of the keratin-PCL composite nanofibers increased greatly with the increase of PCL content. In addition, the compressive strength of electrospun PCL/PEG film-coated 45S5 BG scaffolds (made by foam replication technology) increased significantly, about 2–5 times higher than that of the pure BG scaffold [39]. These

studies have great reference significance for the preparation of keratin/BG hybrid scaffold materials reinforced by using PCL.

Non-toxicity, low immunogenicity, good biocompatibility, biodegradability, porosity and mechanical properties matching with real bone are requirements of composite scaffold materials for bone repair. Considering that keratin has no cytotoxicity, good biocompatibility, biodegradability and easy modification, we proposed to construct a keratin/BG composite scaffold for bone repair by replacing collagen with keratin. In particular, in order to meet the requirements of the appropriate mechanical properties, we first engineered a double cross-linking system, including thiol-ene reaction between keratin and MPTS, and amino-epoxy reaction between keratin and GPTMS, aiming at improving the interface interaction of keratin and BG due to the existence of Si–OH groups derived from Si-OR groups of both MPTS and GPTMS molecules. Secondly, in order to combine the excellent mechanical properties of PCL and the good biocompatibility of keratin to the composite scaffold, PCL was introduced. In this study, porous PCL-keratin-BG composite scaffolds were prepared by in-situ sol–gel method and freeze-drying method. The chemical structure, porous morphology, hydrophilicity, compressive strength and biocompatibility of the prepared scaffolds were characterized and analyzed. The double crosslinking system, especially the thiol-ene reaction aiming at improving the interfacial bonding between keratin and bioactive glass, was systematically studied, and the reinforcement effect of PCL on keratin/BG composite scaffold was discussed in detail. We expect that the idea of PCL to enhance the mechanical strength of keratin-based bone scaffold materials, as well as the strategy of introducing thiol-ene reactions into keratin-based bone scaffold materials using thiol groups in keratin as reaction sites provide theoretical and practical support for the research and development of keratin-based biomedical materials.

2 Materials and methods

2.1 Materials

Keratin and bioactive glass (BG) precursors were prepared by the reduction extraction method from wool and the sol–gel method, respectively. The cytotoxicity of extracted keratin was evaluated, and proved to be non-cytotoxic. Preparation and cytotoxicity evaluation of keratin were shown in 1 and 2 of the Additional file 1. The 3-methacryloxy propyltrimethoxy silane (MPTS), (3-glycidoxymethyl) methyldiethoxysilane (GPTMS), polycaprolactone (PCL, MW ~ 60,000) were purchased from Chengdu Ding sheng Technology Co., Ltd. [3-(4,5-dimethylthiazol-2-yl)-2,5-diphenyltetrazolium bromide (MTT) came from Thermo Fisher Scientific, Inc. The L929 cell line was obtained from the Shanghai Cellular Institute of China Scientific Academy. Sodium hydrogen sulfite and potassium persulfate were supplied by Chengdu Ke Long Technology Co., Ltd. All reagents are used as they were received.

2.2 Fabrication of keratin-BG and PCL-keratin-BG composite scaffolds

For the preparation of keratin-BG composite scaffold, the main processes are conducted as follows. In order to make the click reaction proceed effectively, firstly, the keratin powder was reduced by sodium bisulfite (the procedure for reduction of keratin was provided in 4 of the Additional file 1) so as to obtain a thiol content (e.g. 3.8 mmol/g), then MPTS containing unsaturated double bonds (the same mole as thiol group), and initiator potassium persulfate (50% of thiol content) and sodium bisulfite (the same mole of potassium persulfate) was added to the reduced keratin solution to take the thiol-ene reaction at 50 °C for 15 h. After that, the reaction mixture was dialyzed, and then GPTMS containing epoxy groups (50% of mass of keratin powder) was added for further reaction for 2 h. Subsequently, the BG precursor sol (twice the mass of keratin powder) was added and stirring at 50 °C for 6 h. Finally, the composite mixture was moved to the specific mold and frozen at − 20 °C for 12 h and further freezing dried at − 57 °C for 48 h to obtain the keratin-BG scaffold.

For the PCL-keratin-BG scaffold, except that the PCL solution obtained by dissolving in dichloromethane was added when the reaction proceeded for 2 h after adding BG precursor, the other steps were the same as those of preparing keratin-BG scaffold. The preparation process of the composite scaffold is shown in Fig. 1.

3 Characterization

3.1 Analyses of chemical structure

3.1.1 Fourier transform infrared spectroscopy (FTIR)

Samples of keratin, MTPS, BG, keratin-BG and PCL-keratin-BG were ground separately, pressed together with the KBr crystal, and characterized by FTIR (MAGNA IR560, Nicolet, USA), respectively. The scanning wavenumber ranges from 500 to 4000 cm^{-1}.

3.1.2 ^1H NMR

KH-570 was dissolved in chloroform, keratin and keratin-MPTS were dissolved in D_2O. ^1H NMR measurements were recorded with a Bruker 400 MHz Advance NMR instrument (Bruker AV, Bruker, Switzerland) at 25 °C.

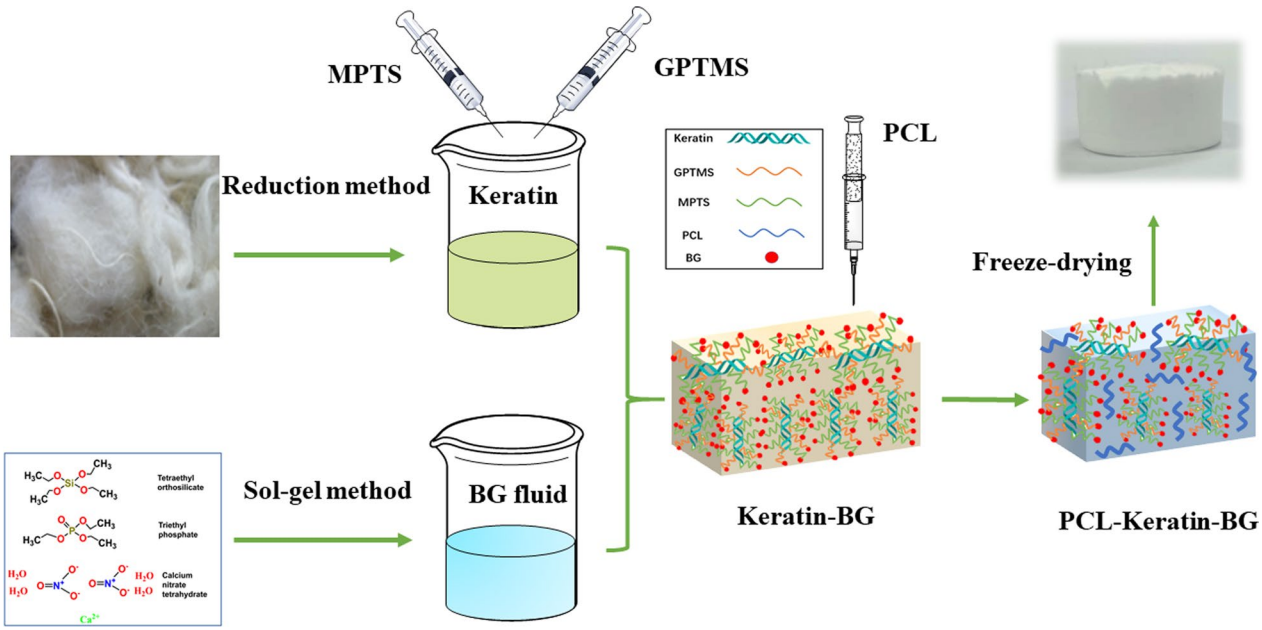

Fig.1 Schematic illustration of preparation of PCL-Keratin-BG composite scaffold

3.2 Morphology observation and porosity detection of scaffolds

3.2.1 Morphology observation

The cross-sectional morphology of scaffolds was observed by an JSM-5900LV(JEOL) scanning electron microscope at 15 kV. Firstly, the sample was brittle broken under liquid nitrogen, and then the cross section was sprayed with gold. The treated samples were put into the instrument to observe the whole picture of the sample under different multiples.

3.2.2 Porosity

Porosity was measured by liquid displacement method [16]. A small square sample of ~ 1 cm^3 was immersed in anhydrous ethanol with a volume of V_1 for 24 h. V_2 was the total volume of the sample and anhydrous ethanol. After the sample was taken out of the measuring tube, the remaining absolute ethanol volume was V_3. The formula (1) for calculating the porosity of the sample is shown below.

$$P = \frac{V1 - V3}{V2 - V3} \times 100\% \quad (1)$$

3.3 Hydrophilicity testing

3.3.1 Contact angle

The surface wettability of the scaffold was analyzed by Video Optical Contact Angle (Dataphysics, Germany). Samples was processed into a rectangular block, and placed in the designated position of the instrument. And 4 μL double distilled water was used as indicator liquid, and 5 different points were selected for each sample to measure. Finally, the average value was acquired.

3.3.2 Water absorption

The water absorption capacity was measured according to the literature [48]. Cutting samples into a 1 cm × 1 cm square and recording its weight as W_1, then soaking it in deionized water and taking it out at different time points. The surface of the square sample was slightly wiped, and then its weight was recorded as W_2. The water absorption rate of the scaffold was calculated according to the following formula (2), and each sample was tested three times to calculate the average value and the variance.

$$W\,(\%) = \frac{(W2 - W1)}{W1} \times 100\% \quad (2)$$

3.4 Mechanical properties

Mechanical properties of the scaffolds were detected by INSTRON 5967 (Instron, USA) at room temperature. In dry state, the cylindrical sample was compressed to 80% at a compression rate of 1 mm/min. Each sample was tested five times in parallel, and the average value was calculated as the final result.

3.5 In vitro biological activity evaluation

3.5.1 In vitro mineralization experiment

Simulated body fluid (SBF) was prepared by the method described in the literature [40]. First, samples were cut into 1×1 cm^2 square, and then put into centrifuge tubes containing SBF, and centrifuge tubes were placed in a shaker at 37 °C for in vitro mineralization. The samples were soaked for 1, 3 and 7 days, then taken out and rinsed 3 times with deionized water. Finally, it was dried at 40 °C, and its mineralization effect in vitro was characterized by SEM and EDS.

3.5.2 In vitro cell culture study

The cytotoxicity of the scaffolds was evaluated in vitro by the MTT assay [35]. L929 fibroblasts were seeded in 96-well tissue plates. Before sterilization, the samples were made into 3×3 square centimeters, and then they were co-cultured with 3 ml of culture medium (Sigma Aldrich) for 1 day. Then, 200 μL of the extractive medium was introduced into the 96-well plastic tissue plates. The culture conditions were kept constant with the temperature of 37 °C, 5% CO_2 and 95% relative humidity. At different time intervals (1 day, 3 days, and 5 days), the cell seeding plates were taken out of the incubator. And 20 μL of MTT was introduced to each well. After incubation for 4 h, blue thyroxine crystals were formed. After dissolving the crystals with dimethyl sulfoxide, the plate was shaken in the dark for 15 min. Finally, absorbance values were measured at a wavelength of 490 nm by using microplate reader (ELX808IU, Bio-Tek, USA).

3.6 Statistical analysis

Samples were used in triplicate for water absorption test, five for porosity, mechanical properties and contact angle measurements, and four for biological experiments (*i.e.* MTT assay). The experimental results were expressed as mean value ± standard deviation (SD). Two-way analysis of variation (ANOVA) was used for statistical analysis using Origin Pro software (Origin Lab Corporation, Northampton, MA, USA). A significant difference between the scaffolds was considered at the *p*-value of less than 0.05 ($p < 0.05$).

4 Results and discussion

4.1 Characterization of chemical structure

4.1.1 Thiol-ene click reaction

For the preparation of keratin-BG and PCL-keratin-BG composite scaffolds, the first step is the modification of keratin with MPTS via thiol-ene click reaction. Figure 2a showed the FTIR spectra of MPTS, keratin and their reaction resultant (keratin-MPTS). The spectrum of keratin showed that the absorption bonds at 3336 cm^{-1}, 1652 cm^{-1}, 1543 cm^{-1}, 1240 cm^{-1} were the characteristic peaks of amide A, amide I, amide II and amide III, respectively [41]. And the characteristic peaks of MPTS were observed at 810 cm^{-1} and 1637 cm^{-1}, which belong to the absorption bands of Si–C and C=C, respectively. In particular, compared with keratin, in the spectrum of keratin-MPTS, the characteristic peaks of Si–C (800 cm^{-1}) appeared, which indicated that the silicone segments of MPTS molecules were introduced to keratin. It can also be found that the stretching vibration peak of the bond C=C (1637 cm^{-1}) was weakened in keratin-MPTS, which indicated that the double bonds participated in the thiol-ene reaction. Furthermore, the peak at 1637 cm^{-1} was widened, which is attributed to that the amide I band of keratin fell the overlapping area of MPTS absorption. Importantly, the C–S–C stretching vibration peak appeared at 1156 cm^{-1}, which indicated that the double bonds of MPTS have really reacted with the thiol

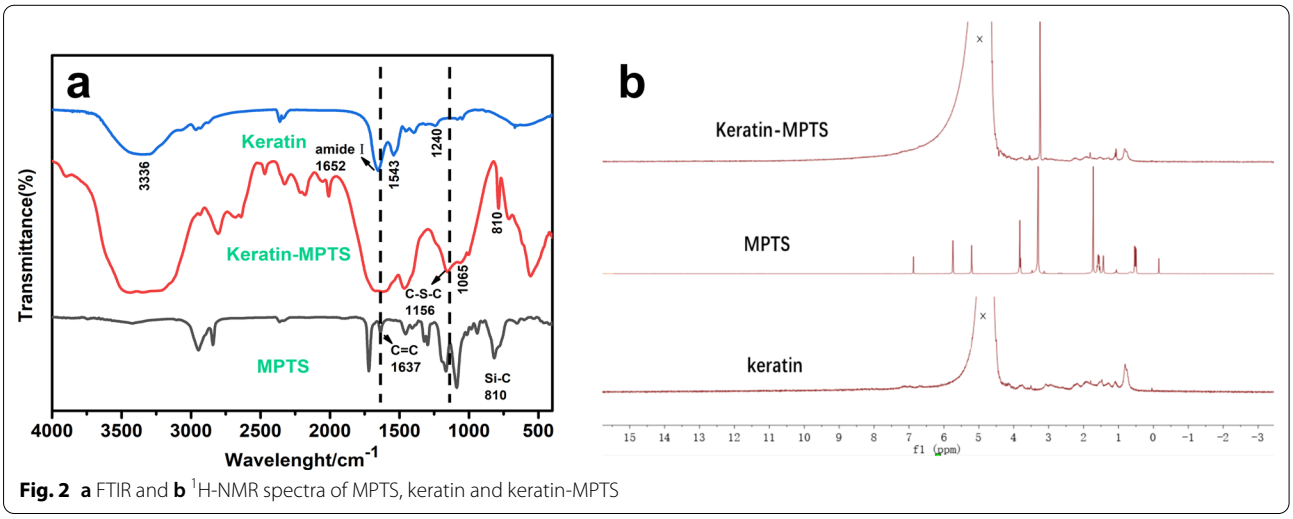

Fig. 2 **a** FTIR and **b** ^{1}H-NMR spectra of MPTS, keratin and keratin-MPTS

groups in keratin. These results indicated that the thiol-ene reaction of keratin and MPTS has been successfully carried out.

In addition, the success of the thiol-ene reaction was further confirmed by ^{1}H NMR characterization (Fig. 2b). In the ^{1}H NMR spectrum of keratin-MPTS, the peak at 3.58 ppm was attributed to the protons of $-CH_2-CH_2-O-$ of MPTS, which is obviously due to the success of the thiol-ene click reaction of MPTS and keratin [28]. Besides, the signal at 4.7 ppm was ascribed to D_2O.

4.1.2 Structure of keratin-BG and PCL-keratin-BG composites

From the FTIR spectrum of keratin (Fig. 3), it can be seen that a broad peak appeared at 3336 cm^{-1}, which may be caused by the overlapping of $-NH_2$ and $-OH$ groups. However, in the spectrum of keratin-BG (Fig. 3), the peaks of stretching vibration peak of $-OH$ (3442 cm^{-1}) and $-NH_2$ (3349 cm^{-1}) were clearly separated, and the peak intensity of $-OH$ increased, but that of $-NH_2$ displayed a tendency to decrease. This phenomenon is probably the reason that the increase of peak intensity of $-OH$ groups may be caused by the introduction of BG, and the decrease of that of $-NH_2$ may be caused by the reaction of $-NH_2$ with the epoxy group in GPTMS [16]. The peaks at 789 cm^{-1} and 1075 cm^{-1} in the keratin-BG scaffold or PCL-keratin-BG were attributed to the asymmetric stretching vibration of Si–O–Si bonds, which may be mainly due to the condensation between the Si–OH groups in BG and the Si–OH groups in MPTS or GPTMS [42]. Furthermore, the bands at 2924 cm^{-1} and 2856 cm^{-1} that ascribed to asymmetric and symmetric stretching vibration of $-CH_2-$ respectively [17], that appeared in the FTIR spectrum of PCL and PCL-keratin-BG as well (Fig. 3), which indicated that polycaprolactone was successfully introduced into the keratin-BG composite [38].

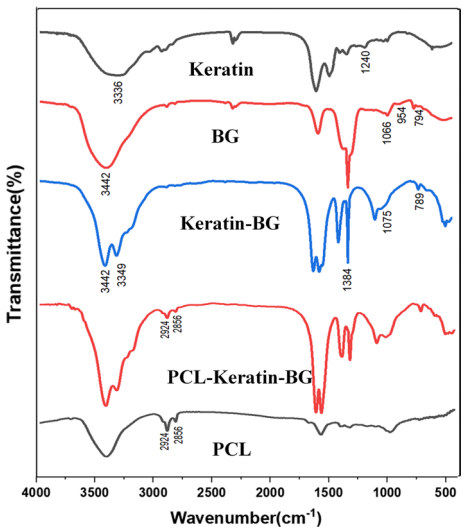

Fig. 3 FTIR spectra of BG, PCL, and keratin-BG and PCL-keratin-BG composites

4.2 Porous morphology of keratin-BG and PCL-keratin-BG scaffolds

Composite scaffolds for bone repair play an important role in creating space for the adhesion, growth and proliferation of osteoblast cells and to provide channels for the transportation of nutrients and metabolic wastes during the repair of damaged or diseased bones. Interconnected pore structure is conducive to the adhesion and proliferation of cells. It can be seen from the SEM images (Fig. 4a, b) that both the keratin-BG and PCL-keratin-BG scaffolds showed the interconnected porous structure. Especially, the surface of keratin-BG scaffold (Fig. 4a) was smoother, and the distribution of BG in the scaffold material was more uniform, which indicated that the compatibility between keratin and BG was better. This phenomenon may be explained as follows: on the one hand, the epoxy groups of the GPTMS could react with the amino groups in keratin to form covalent bonds, which is similar to gelatin-BG composite prepared by introducing GPTMS reported by Gao [16] and Ziba Orshesh [32]; and the sulfhydryl groups of keratin could react with the C=C bonds of MPTS through thiol-ene reaction. On the other hand, the hydrogen bonds would be formed, or co-condensation between the Si–OH groups of BG and the Si–OH groups of GPTMS or MPTS would lead to form Si–O–Si bonds. As for the PCL-keratin-BG scaffold (Fig. 4b), a tightly packed structure was observed, which increased the roughness of the scaffold and would facilitate cell adhesion [54]. In Fig. 4c, d, the keratin-BG and PCL-keratin-BG scaffolds showed the pore size range mainly concentrated in 65–165 μm and 100–220 μm, and the average pore diameter (Fig. 4e) about 126 ± 23.6 μm and 153 ± 27.8 μm, respectively. Many researchers determined the range to be above 100 μm when searching for the ideal pore size. The average size of the human bone unit is 223 μm [43]. Clearly, the pore size fell within the size range (around 100–200 μm), which is favorable for cell proliferation and growth [16, 44]. In addition, after the introduction of polycaprolactone, the porosity (Fig. 4e) of the PCL-keratin-BG scaffold decreased from $83.08 \pm 3.2\%$ of keratin-BG scaffold to $72.12 \pm 1.79\%$, which may be due to hydrophobicity of PCL. Nevertheless, the porosity of PCL-keratin-BG is still more than 70%, which could provide enough space for cell migration, proliferation and nutrient transfer [45, 46].

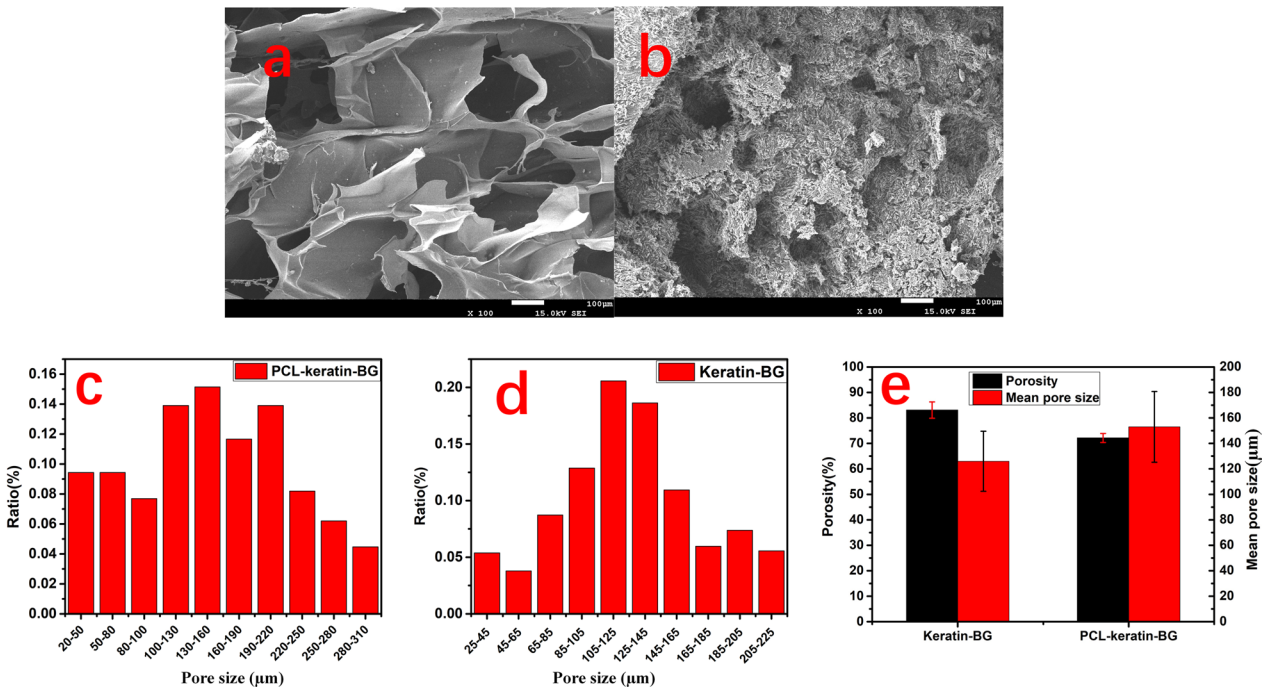

Fig. 4 SEM images and pore size distribution of (**a**, **c**) keratin-BG and (**b**, **d**) PCL-keratin BG, respectively, (**e**) porosity and mean pore size of keratin-BG and PCL-keratin-BG

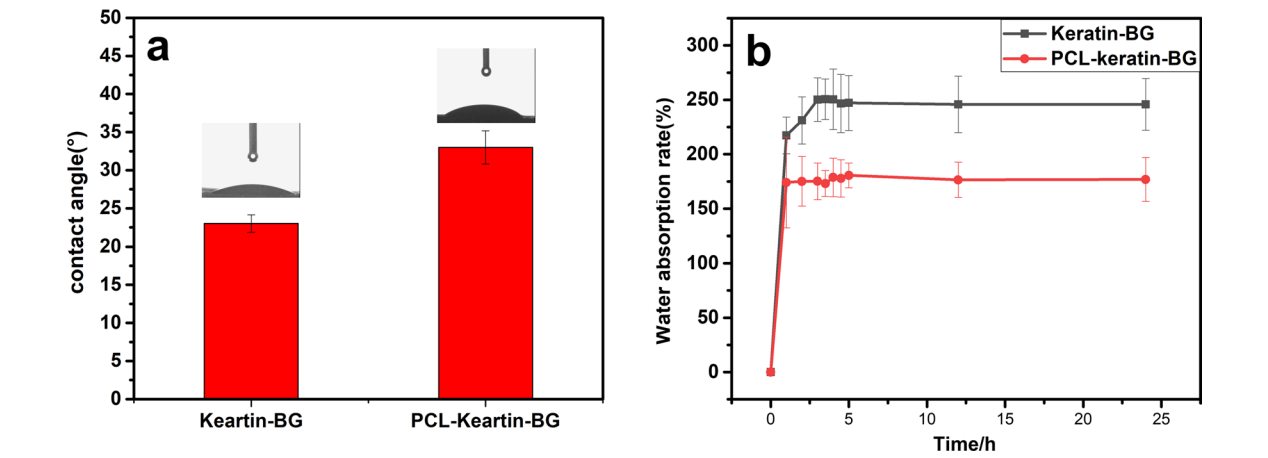

Fig. 5 **a** Contact angle and **b** water absorption rate of keratin-BG and PCL-keratin-BG

4.3 Hydrophilicity of scaffolds

Hydrophilicity is one of the important characteristics of tissue engineering scaffolds, which could enhance the cell attachment, proliferation, migration and vitality. The smaller the water contact angle is, the stronger the hydrophilicity of the material surface is, and vice versa. Figure 5a showed that the contact angle of keratin-BG scaffold material was 21.4 ± 1.14°, showing excellent hydrophilicity. This is likely due to that keratin is hydrophilic biomaterial containing many hydrophilic groups such as amino and carboxyl groups, and bioactive glass contains lots of hydrophilic hydroxyl groups [47]. On the contrary, PCL is hydrophobic material, which reduces the hydrophilicity and increases the contact angle of the scaffold. As a result, the contact angle of the PCL-keratin-BG scaffold (31.8 ± 4.7°) increased slightly, which still maintained excellent hydrophilicity. The results indicated that the PCL-keratin-BG scaffold

possessed good surface wettability, which is beneficial to cell adhesion and proliferation. Furthermore, as shown in Fig. 5b, both scaffolds showed rapid water absorption when immersed in water. Especially, the water absorption rate of keratin-BG and PCL-keratin-BG scaffolds gradually stabilized after 2.5 h and 3.5 h, and finally remained at 245.7 ± 23.7% and 176.8 ± 20.2%, respectively. Although the water absorption rate of the PCL-keratin-BG scaffold was lower than that of the keratin-BG scaffold due to its lower porosity [22] and hydrophobicity of introduction of PCL, the PCL-keratin-BG scaffold was of still benefit to the cell attachment, proliferation and migration.

4.4 Mechanical properties

The bone repair composite scaffold must provide certain mechanical support during the bone regeneration process to keep the tissue from deforming. In general, PCL is used to improve the mechanical strength of biomedical materials because it has excellent mechanical properties [48–50]. In this study, the dual cross-linking system containing thiol-ene and amino-epoxy reaction at the same time was selected (as shown in 5 of the Additional file 1) along with the introduction of polycaprolactone (PCL) were used to enhance the mechanical properties of the PCL-keratin-BG scaffold. Mechanical properties such as compressive strength and Young's modulus of the keratin-BG and PCL-keratin-BG scaffold were measured (Fig. 6a). The average compressive strength and average Young's modulus of the keratin-BG scaffold were 0.91 ± 0.06 MPa and 7.25 ± 1.7 MPa, respectively. However, PCL-keratin-BG after introducing PCL showed increased average compressive strength (1.58 ± 0.21 MPa) and enhanced average Young's modulus (14.14 ± 1.95 MPa), which indicated that it meets the requirement of cancellous bone (compressive strength 1–10 MPa). As shown in the stress–strain curves (Fig. 6b), the PCL-keratin-BG scaffold can withstand greater pressure under the same displacement in comparison with the keratin-BG scaffold, which is just as we expected. In addition, compared with the keratin-BG scaffold, the low porosity of the PCL-keratin-BG scaffold may be also one of the reasons for its high mechanical strength [51]. As compared with the compressive strength of scaffolds for bone regeneration reported in literature, such as the biomineralized keratin/HA scaffold (0.778 MPa) [48], and PCL/BG-SA/Gel scaffold (1.44 MPa) [4], the PCL-keratin-BG scaffold possessed relative stronger mechanical properties, which further indicated that its potential to the application of regeneration of cancellous bone.

4.5 In vitro mineralization characterization

Ion concentration in simulated body fluid (SBF) is almost similar to that in human blood. After immersion in a simulated body fluid, the detection of apatite formation on the scaffold surface is a standard for evaluating the bone conductivity of the scaffold [52]. As shown in Fig. 7, with the increase of mineralization days, the amount of crystals formed on the surfaces of two scaffolds increased. From Table 1 and EDS inserted in Fig. 7, it can be seen that the calcium/phosphorus ratio of the obtained crystals was close to 1.67, which is consistent with the calcium-phosphorus ratio of natural hydroxyapatite. The results suggested that, as expected, hydroxyapatite was formed on the scaffold surface after mineralization in simulated body fluids. Furthermore, compared with the keratin-BG, the introduction of PCL to PCL-keratin-BG had a slight negative effect on the production of

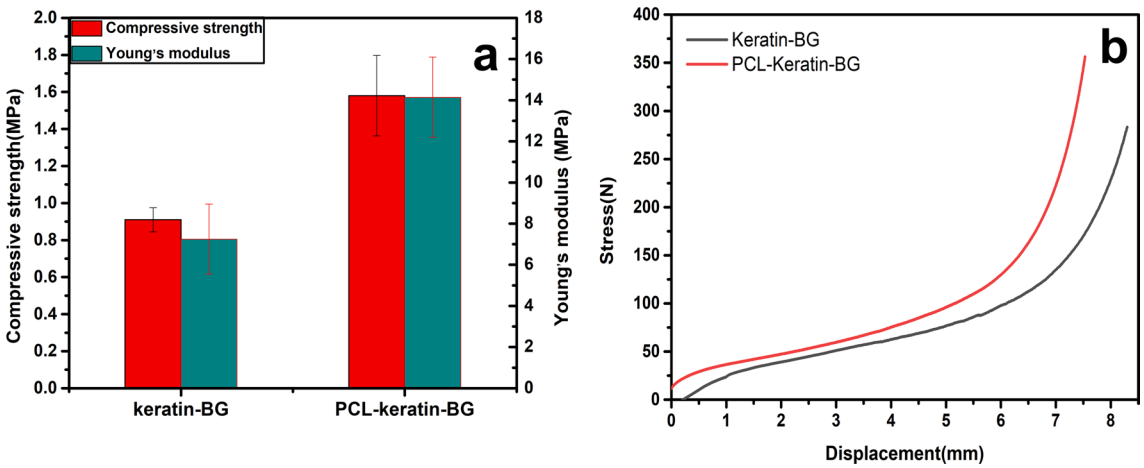

Fig. 6 **a** Compressive strength, Young's modulus and **b** stress-displacement curves of keratin-BG and PCL-keratin-BG

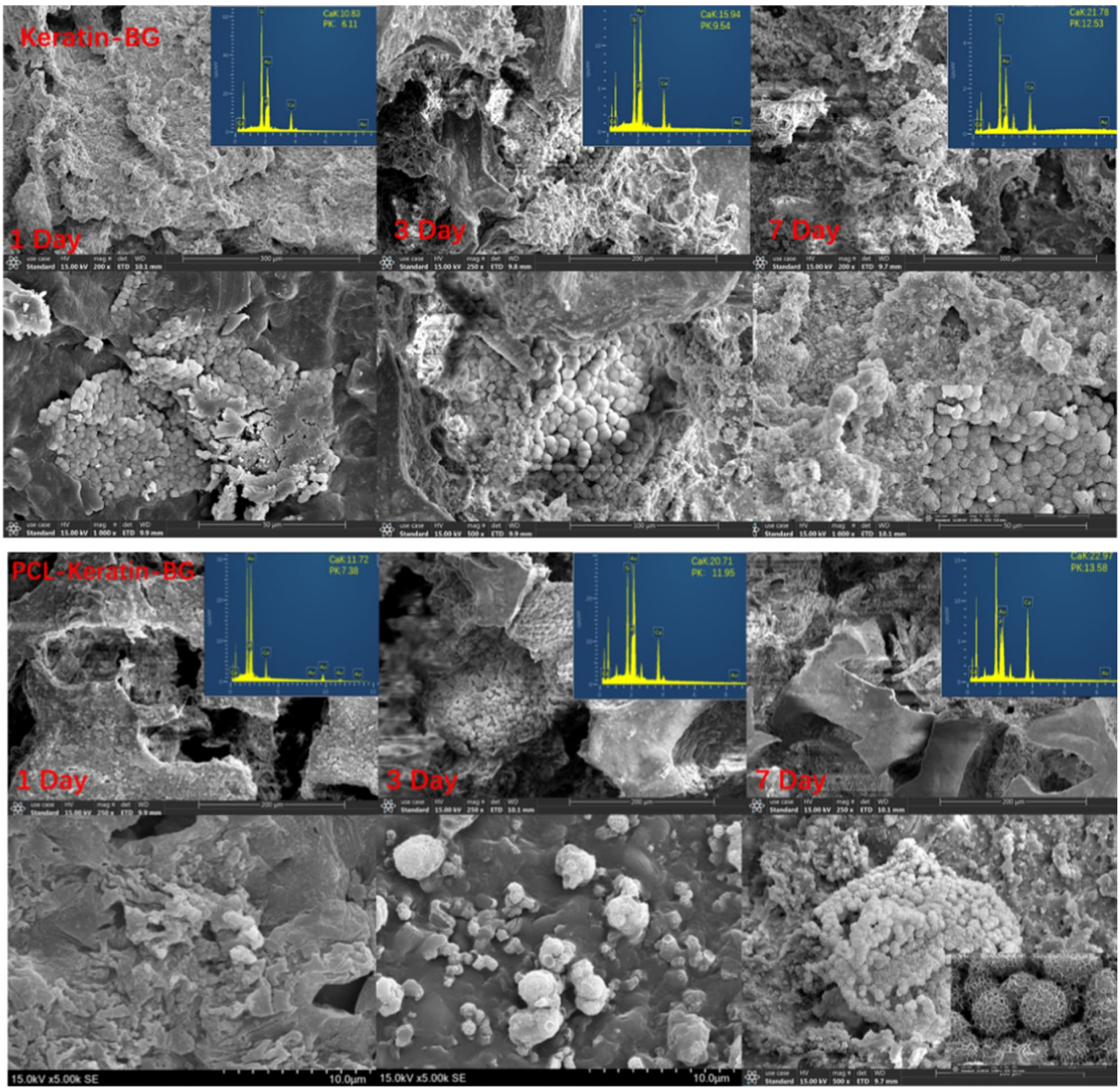

Fig. 7 SEM images of keratin-BG and PCL-keratin-BG scaffolds immersed in simulated body fluid for 1, 3, and 7 days

hydroxyapatite. The reason may be that the hydroxyapatite layer is easily to form on the surface of the bioactive glass through interactions, while hydroxyapatite cannot be produced on the pure PCL scaffold or scaffold without bioactive inorganic component (such as CaP) [34]. Importantly, keratin has a large number of hydrophilic active groups, such as carboxyl, which is beneficial to the deposition of inorganic minerals such as calcium carbonate and calcium phosphate and plays an important role in mineralization. In addition, the amino acid residues in keratin, such as aspartic acid, glycine and serine, could modulate the mineralization [53, 54]. It is worth noting that after biomineralization for 7 days, the surface of the two scaffolds were almost covered by hydroxyapatite,

Table 1 The radio of calcium to phosphorus (Ca/P) of HA after mineralization in keratin-BG and PCL-keratin-BG scaffolds

	Day 1	Day 3	Day 7
Keratin-BG	1.77	1.67	1.73
PCL-keratin-BG	1.59	1.73	1.69

which proved that the keratin-BG scaffold and PCL-keratin-BG scaffold have excellent mineralization ability, suggesting that they would play a positive effect on inducing bone regeneration.

4.6 Biocompatibility–cell viability assay

Composite scaffold materials for bone repair should be non-toxic, non-teratogenic, favorable for cell adhesion and provide a good growth microenvironment. MTT method and CCK-8 method can reflect the cytotoxicity of scaffold by detecting the survival and proliferation of cells in the leaching solution of the scaffold material or on the scaffold surface [15]. In this study, the MTT assay was used to detect the growth of L929 mouse fibroblasts in the extracts of keratin-BG scaffold and PCL-keratin-BG scaffold. The results (Fig. 8) showed that, compared with the negative control group (containing medium and cells), two kinds of scaffold materials were not only non-toxic, but also had a certain promotion effect on cell growth and proliferation. The OD values of the keratin-BG scaffold and the PCL-keratin-BG scaffold are almost the same on day 1, day 3, day 5, illustrating that PCL has only little effect on the cytotoxicity of the scaffold [55]. During the process of cell growth, the cell growth rate from the 3rd day to the 5th day was slower than that from the first day to the 3rd day. This may be due to the insufficient space and nutrients, which restricted cell proliferation. On the 5th Day, the porosity of the PCL-keratin-BG scaffold was slightly lower than that of the keratin-BG scaffold, which makes the OD value of the PCL-keratin-BG scaffold lower than that of the keratin-BG scaffold. This was consistent with WU's research on the viability of cells [47]. Relative growth rate (RGR) and cytotoxicity grade were calculated and shown in 6 of the Additional file 1. Both scaffolds have almost no cytotoxicity, and both of them reach grade 0, which meets the in vivo use standard.

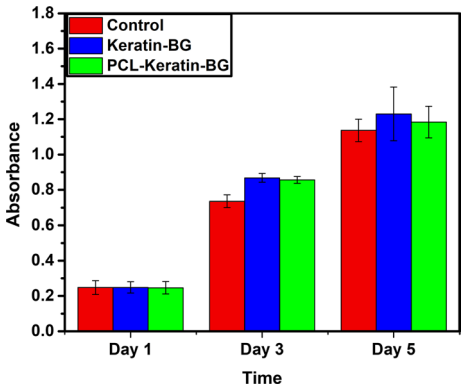

Fig. 8 In vitro cytotoxicity evaluation of cells in contact with scaffold materials for 1, 3, and 5 days

5 Conclusion

In this paper, both keratin-BG scaffold and PCL strengthening PCL-keratin-BG composite scaffold with double cross-linked network structure were prepared by in situ sol–gel process and freeze-drying method. Firstly, FTIR and ^{1}H-NMR analyses proved the success of the thiol-ene click reaction between rich sulfhydryl groups of keratin and the unsaturated double bond of MPTS. Secondly, keratin, BG, PCL, and keratin-BG and PCL-keratin-BG composite scaffolds were characterized via the FTIR and XRD, which showed that the PCL-keratin-BG composite scaffold was successfully prepared. Subsequently, the SEM observation showed that keratin-BG and PCL-keratin-BG had interconnected pore structure and suitable average pore size (153 μm ± 27.8). Water absorption and water contact angle measurements demonstrated they had good wettability. These results are more conducive to the adhesion, growth and proliferation of bone cells. In particular, compression test results showed that the double cross-linked network formed by the both thiol-ene reaction and amino-epoxy group reaction, together with the introduction of polycaprolactone can improve mechanical properties of the composite scaffolds. In addition, both the biomineralization experiment and cytotoxicity test (MTT assay) manifested that the introduction of PCL has only negligible negative effect on the biological properties of the composite scaffolds, and showed PCL-keratin-BG composite scaffold has almost no-cytotoxicity. Therefore, PCL-keratin-BG composite scaffold prepared by using the strategy proposed in this study has great potential to be applied in bone repair field.

Abbreviations

PCL: Polycaprolactone; BG: Bioactive glass; MPTS: 3-Methacryloxy propyltrimethoxy silane; GPTMS: (3-Glycidoxymethyl) methyldiethoxysilane; CNC: Cellulose nanocrystals; MTT: [3-(4,5-Dimethylthiazol-2-yl)-2,5-diphenyl-tetrazolium bromide; LDV: Leucine-aspartic acid-valine; EDS: Glutamate-aspartic acid-serine; PHB: Poly(3-hydroxybutyrate); PLA: Polylactic acid; PG1CL: Poly(globalide-*co*-ε-caprolactone); Gel: Gelatin; MPEGMA: Poly(ethylene glycol) methyl ether methacrylate.

Supplementary Information

The online version contains supplementary material available at https://doi.org/10.1186/s42825-021-00077-w.

Additional file 1: The main results of extraction of keratin from wool, evaluation of cytotoxicity of keratin, synthesis of bioactive glass precursor, reduction of keratin, selection of double cross-linking system and toxicity levels of Keratin-BG and PCL-Keratin-BG.

Acknowledgements
Thanks for the support of the National Natural Science Foundation of China (No. 21376153) and the Fundamental Research Funds for the Central University.

Authors' contributions
ZL made substantial contributions to conception and design of this review and critically revised the article for important intellectual content. LS collected and summarized references, completed the experiment and wrote this manuscript. All authors read and approved the final manuscript.

Funding
National Natural Science Foundation of China (No. 21376153); Fundamental Research Funds for the Central University.

Availability of data and materials
All data generated or analysed during this study are included in this published article, and Additional file 1.

Declarations

Competing interests
The authors declare that they have no competing interests.

Author details
[1]National Engineering Research Center of Clean Technology in Leather Industry, Sichuan University, Chengdu, China. [2]Key Laboratory of Leather Chemistry and Engineering of Ministry of Education, Sichuan University, Chengdu, China.

Received: 9 March 2021 Accepted: 10 November 2021
Published online: 15 January 2022

References

1. Aragon J, Salerno S, De Bartolo L, Irusta S, Mendoza G. Polymeric electrospun scaffolds for bone morphogenetic protein 2 delivery in bone tissue engineering. J Colloid Interface Sci. 2018;531:126–37.
2. Goonoo N, Khanbabaee B, Steuber M, Bhaw-Luximon A, Jonas U, Pietsch U, Jhurry D, Schonherr H. kappa-Carrageenan enhances the biomineralization and osteogenic differentiation of electrospun polyhydroxybutyrate and polyhydroxybutyrate valerate fibers. J Biomacromol. 2017;18(5):1563–73.
3. Fan B, Wang X, Zhang H. Improving the osteogenesis and degradability of biomimetic hybrid materials using a combination of bioglass and collagen I. J Mater Des. 2016;112:67–79.
4. Mao D, Li Q, Li D, Tan Y, Che Q. 3D porous poly(ε-caprolactone)/58S bioactive glass–sodium alginate/gelatin hybrid scaffolds prepared by a modified melt molding method for bone tissue engineering. J Mater Des. 2018;160:1–8.
5. Zhang D, Wu X, Chen J, Lin K. The development of collagen based composite scaffolds for bone regeneration. J Bioact Mater. 2018;3(1):129–38.
6. Hernandez-Gonzalez AC, Tellez-Jurado L, Rodriguez-Lorenzo LM. Alginate hydrogels for bone tissue engineering, from injectables to bioprinting: a review. J Carbohydr Polym. 2020;229:115514.
7. Abinaya B, Prasith TP, Ashwin B, Viji Chandran S, Selvamurugan N. Chitosan in surface modification for bone tissue engineering applications. J Biotechnol. 2019;14(12):e1900171.
8. Zhang XY, Chen YP, Han J, Mo J, Dong PF, Zhuo YH, Feng Y. Biocompatiable silk fibroin/carboxymethyl chitosan/strontium substituted hydroxyapatite/cellulose nanocrystal composite scaffolds for bone tissue engineering. J Int J Biol Macromol. 2019;136:1247–57.
9. Liu M, Zheng H, Zhou C. Chitosan-chitin nanocrystal composite scaffolds for tissue engineering. Carbohydr Polym. 2016;152:832–40.
10. Gregor A, Filova E, Novak M, Kronek J, Chlup H, Buzgo M, Blahnova V, Lukasova V, Bartos M, Necas A, Hosek J. Designing of PLA scaffolds for bone tissue replacement fabricated by ordinary commercial 3D printer. J Biol Eng. 2017;11:31.
11. Park SA, Lee SJ, Seok JM, Lee JH, Kim WD, Kwon IK. Fabrication of 3D printed PCL/PEG polyblend scaffold using rapid prototyping system for bone tissue engineering application. J Bionic Eng. 2018;15(3):435–42.
12. Gentile P, Chiono V, Carmagnola I, Hatton PV. An overview of poly(lactic-co-glycolic) acid (PLGA)-based biomaterials for bone tissue engineering. Int J Mol Sci. 2014;15(3):3640–59.
13. Dwivedi R, Kumar S, Pandey R, Mahajan A, Nandana D, Katti DS, Mehrotra D. Polycaprolactone as biomaterial for bone scaffolds: review of literature. J Oral Biol Craniofac Res. 2020;10(1):381–8.
14. Carlström IE, Rashad A, Campodoni E, Sandri M, Syverud K, Bolstad AI, Mustafa K. Cross-linked gelatin-nanocellulose scaffolds for bone tissue engineering. J Mater Lett. 2020;264:127326.
15. Dehnavi N, Parivar K, Goodarzi V, Salimi A, Nourani MR. Systematically engineered electrospun conduit based on PGA/collagen/bioglass nanocomposites: the evaluation of morphological, mechanical, and bioproperties. Polym Adv Technol. 2019;30(9):2192–206.
16. Gao W, Sun L, Zhang Z, Li Z. Cellulose nanocrystals reinforced gelatin/bioactive glass nanocomposite scaffolds for potential application in bone regeneration. J Biomater Sci Polym Ed. 2020;31(8):984–98.
17. Gautam S, Sharma C, Purohit SD, Singh H, Dinda AK, Potdar PD, Chou CF, Mishra NC. Gelatin-polycaprolactone-nanohydroxyapatite electrospun nanocomposite scaffold for bone tissue engineering. J Mater Sci Eng C Mater Biol Appl. 2021;119:111588.
18. Luo J, Zhu J, Wang L, Kang J, Wang X, Xiong J. Co-electrospun nano-/microfibrous composite scaffolds with structural and chemical gradients for bone tissue engineering. J Mater Sci Eng C Mater Biol Appl. 2021;119:111622.
19. Declercq HA, Desmet T, Berneel EE, Dubruel P, Cornelissen MJ. Synergistic effect of surface modification and scaffold design of bioplotted 3-D poly-epsilon-caprolactone scaffolds in osteogenic tissue engineering. J Acta Biomater. 2013;9(8):7699–708.
20. Zhang C, Xia L, Zhang J, Liu X, Xu W. Utilization of waste wool fibers for fabrication of wool powders and keratin: a review. J Leather Sci Eng. 2020. https://doi.org/10.1186/s42825-020-00030-3.
21. Wang Y, Zhang W, Yuan J, Shen J. Differences in cytocompatibility between collagen, gelatin and keratin. J Mater Sci Eng C Mater Biol Appl. 2016;59:30–4.
22. Arslan YE, Sezgin Arslan T, Derkus B, Emregul E, Emregul KC. Fabrication of human hair keratin/jellyfish collagen/eggshell-derived hydroxyapatite osteoinductive biocomposite scaffolds for bone tissue engineering: From waste to regenerative medicine products. J Colloids Surf B Biointerfaces. 2017;154:160–70.
23. Naderi P, Zarei M, Karbasi S, Salehi H. Evaluation of the effects of keratin on physical, mechanical and biological properties of poly(3-hydroxybutyrate) electrospun scaffold: Potential application in bone tissue engineering. J Eur Polym J. 2020;124:109502.
24. Kim BS, Park KE, Park WH, Lee J. Fabrication of nanofibrous scaffold using a PLA and hagfish thread keratin composite; its effect on cell adherence, growth, and osteoblast differentiation. J Biomed Mater. 2013;8(4):045006.
25. Yu D, Cai JY, Church JS, Wang L. Modifying surface resistivity and liquid moisture management property of keratin fibers through thiol-ene click reactions. J ACS Appl Mater Interfaces. 2014;6(2):1236–42.
26. Ye X, Yuan J, Jiang Z, Wang S, Wang P, Wang Q, Cui L. Thiol-ene photoclick reaction: an eco-friendly and facile approach for preparation of MPEG-g-keratin biomaterial. J Eng Life Sci. 2019;20(1–2):17–25.
27. Guindani C, Frey ML, Simon J, Koynov K, Schultze J, Ferreira SRS, Araujo PHH, de Oliveira D, Wurm FR, Mailander V, Landfester K. Covalently binding of bovine serum albumin to unsaturated poly(globalide-co-epsilon-caprolactone) nanoparticles by thiol-ene reactions. J Macromol Biosci. 2019;19(10):e1900145.
28. Li Q, Zhu L, Liu R, Huang D, Jin X, Che N, Li Z, Qu X, Kang H, Huang Y. Biological stimuli responsive drug carriers based on keratin for triggerable drug delivery. J Mater Chem. 2012;22(37):19964.
29. Taveri G, Hanzel O, Sedláček J, Toušek J, Neščaková Z, Michálek M, Dlouhý I, Hnatko M. Consolidation of Bioglass® 45S5 suspension through cold isostatic pressing. J Ceram Int. 2021;47(3):4090–6.
30. Schatkoski VM, Larissa do Amaral Montanheiro T, Canuto de Menezes BR, Pereira RM, Rodrigues KF, Ribas RG, Morais da Silva D, Thim GP. Current advances concerning the most cited metal ions doped bioceramics and

silicate-based bioactive glasses for bone tissue engineering. J Ceram Int. 2021;47(3):2999–3012.
31. Delpino GP, Borges R, Zambanini T, Joca JFS, Gaubeur I, de Souza ACS, Marchi J. Sol–gel-derived 58S bioactive glass containing holmium aiming brachytherapy applications: a dissolution, bioactivity, and cytotoxicity study. J Mater Sci Eng C Mater Biol Appl. 2021;119:111595.
32. Orshesh Z, Borhan S, Kafashan H. Physical, mechanical and in vitro biological evaluation of synthesized biosurfactant-modified silanated-gelatin/sodium alginate/45S5 bioglass bone tissue engineering scaffolds. J J Biomater Sci Polym Ed. 2020;31(1):93–109.
33. Lim J, You M, Li J, Li Z. Emerging bone tissue engineering via Polyhydroxyalkanoate (PHA)-based scaffolds. J Mater Sci Eng C Mater Biol Appl. 2017;79:917–29.
34. Zhao X, Lui YS, Choo CKC. Calcium phosphate coated Keratin-PCL scaffolds for potential bone tissue regeneration. J Mater Sci Eng C Mater Biol Appl. 2015;49:746–53.
35. Boakye MAD, Rijal NP, Adhikari U, Bhattarai N. Fabrication and characterization of electrospun PCL-MgO-keratin-based composite nanofibers for biomedical applications. J Mater (Basel). 2015;8(7):4080–95.
36. Cruz-Maya I, Guarino V, Almaguer-Flores A, Alvarez-Perez MA, Varesano A, Vineis C. Highly polydisperse keratin rich nanofibers: Scaffold design and in vitro characterization. J Biomed Mater Res A. 2019;107(8):1803–13.
37. Edwards A, Jarvis D, Hopkins T, Pixley S, Bhattarai N. Poly(epsilon-caprolactone)/keratin-based composite nanofibers for biomedical applications. J Biomed Mater Res B Appl Biomater. 2015;103(1):21–30.
38. Li Y, Wang Y, Ye J, Yuan J, Xiao Y. Fabrication of poly(epsilon-caprolactone)/keratin nanofibrous mats as a potential scaffold for vascular tissue engineering. J Mater Sci Eng C Mater Biol Appl. 2016;68:177–83.
39. Shi Q, Li Z-Y, Liverani L, Roether J, Chen Q, Boccaccini AR. Positive effect of wrapping poly caprolactone/polyethylene glycol fibrous films on the mechanical properties of 45S5 bioactive glass scaffolds. Int J Appl Ceram Technol. 2018;15(4):921–9.
40. Kokubo T, Takadama H. How useful is SBF in predicting in vivo bone bioactivity. J Biomater. 2006;27(15):2907–15.
41. Li J-S, Li Y, Liu X, Zhang J, Zhang Y. Strategy to introduce an hydroxyapatite–keratin nanocomposite into a fibrous membrane for bone tissue engineering. J Mater Chem B. 2013;1(4):432–7.
42. Gao C, Gao Q, Li Y, Rahaman MN, Teramoto A, Abe K. In vitroevaluation of electrospun gelatin-bioactive glass hybrid scaffolds for bone regeneration. J Appl Polym Sci. 2013;127(4):2588–99.
43. Flautre B, Descamps M. Porous HA ceramic for bone replacement: role of the pores and interconnections experimental study in the rabbit. J Mater Sci Mater Med. 2001;12:679–82.
44. Nadeem D, Kiamehr M, Su B. Fabrication and in vitro evaluation of a sponge-like bioactive-glass/gelatin composite scaffold for bone tissue engineering. J Mater Sci Eng C Mater Biol Appl. 2013;33(5):2669–78.
45. Zhu Y, Zhu R, Ma J, Weng Z, Wang Y, Shi X, Li Y, Yan X, Dong Z, Xu J, Tang C. In vitro cell proliferation evaluation of porous nano-zirconia scaffolds with different porosity for bone tissue engineering. J Biomed Mater. 2015;10(5):055009.
46. Danilevicius P, Georgiadi L, Pateman CJ, Claeyssens F, Chatzinikolaidou M, Farsari M. The effect of porosity on cell ingrowth into accurately defined, laser-made, polylactide-based 3D scaffolds. J Appl Surf Sci. 2015;336:2–10.
47. Wu P, Dai X, Chen K, Li R, Xing Y. Fabrication of regenerated wool keratin/polycaprolactone nanofiber membranes for cell culture. J Int J Biol Macromol. 2018;114:1168–73.
48. Zhang Y, Yu W, Ba Z, Cui S, Wei J, Li H. 3D-printed scaffolds of mesoporous bioglass/gliadin/polycaprolactone ternary composite for enhancement of compressive strength, degradability, cell responses and new bone tissue ingrowth. Int J Nanomed. 2018;13:5433–47.
49. Wang S, Yang Y, Koons GL, Mikos AG, Qiu Z, Song T, Cui F, Wang X. Tuning pore features of mineralized collagen/PCL scaffolds for cranial bone regeneration in a rat model. J Mater Sci Eng C Mater Biol Appl. 2020;106:110186.
50. Huang H-Y, Fan F-Y, Shen Y-K, Wang C-H, Huang Y-T, Chern M-J, Wang Y-H, Wang L. 3D poly-ε-caprolactone/graphene porous scaffolds for bone tissue engineering. J Colloids Surf A Physicochem Eng Asp. 2020;606:12539.
51. Fan J, Yu MY, Lei TD, Wang YH, Cao FY, Qin X, Liu Y. In vivo biocompatibility and improved compression strength of reinforced keratin/hydroxyapatite scaffold. J Tissue Eng Regen Med. 2018;15(2):145–54.
52. Mondal T, Sunny MC, Khastgir D, Varma HK, Ramesh P. Poly(L-lactide-co-Є caprolactone) microspheres laden with bioactive glass-ceramic and alendronate sodium as bone regenerative scaffolds. J Mater Sci Eng C. 2012;32(4):697–706.
53. Fan C, Li J, Xu G, He H, Ye X, Chen Y, Sheng X, Fu J, He D. Facile fabrication of nano-hydroxyapatite/silk fibroin composite via a simplified coprecipitation route. J Mater Sci. 2010;45(21):5814–9.
54. Nakata R, Osumi Y, Miyagawa S, Tachibana A, Tanabe T. Preparation of keratin and chemically modified keratin hydrogels and their evaluation as cell substrate with drug releasing ability. J Biosci Bioeng. 2015;120(1):111–6.
55. Bayati V, Abbaspour MR, Dehbashi FN, Neisi N, Hashemitabar M. A dermal equivalent developed from adipose-derived stem cells and electrospun polycaprolactone matrix: an in vitro and in vivo study. J Anat Sci Int. 2017;92(4):509–20.

Publisher's Note